Environmental Microbiology

ENVIRONMENTAL MICROBIOLOGY

RESEARCH ARTICLE OPEN ACCESS

Environmental Heterogeneity Drives Ecological Differentiation in *Vibrio* Populations Across Subtropical Marine Habitats

Siu Hei Wan | Yangbing Xu | Wenqian Xu | Shara K. K. Leung | Erin Y. N. Yu | Charmaine C. M. Yung

Department of Ocean Science, The Hong Kong University of Science and Technology, Hong Kong, Hong Kong SAR

Correspondence: Charmaine C. M. Yung (ccmyung@ust.hk)

Received: 9 March 2025 | **Revised:** 8 April 2025 | **Accepted:** 28 April 2025

Funding: This work was supported by the Research Grants Council of Hong Kong, AoE/P-601/23-N.

Keywords: coastal ecosystem | metabarcoding | microbial ecology | niche partitioning | *vibrio*

ABSTRACT

Elucidating how environmental gradients structure bacterial communities remains fundamental to microbial ecology. We investigated *Vibrio* population dynamics across contrasting subtropical marine environments in Hong Kong over a year period. Using an integrated approach combining cultivation techniques with molecular analyses of Hsp60 and 16S rRNA genes, we characterised the population structure between a coastal site (Clear Water Bay) and an estuarine site (Deep Bay). The estuarine environment consistently harboured higher *Vibrio* abundances (10^4–10^7 copies/mL) compared to coastal waters (10^2–10^4 copies/mL), with significantly greater phylogenetic diversity. Multivariate analyses revealed salinity as the primary driver of community differentiation between sites, while temperature governed seasonal succession patterns. Phylogenetic analysis of 1521 *Vibrio* isolates identified three distinct ecological groups corresponding to specific temperature-salinity niches, with evidence of habitat-specific thermal adaptations among closely related strains. Experimental characterisation of thermal performance curves confirmed physiological differentiation between warm- and cool-temperature adapted strains despite high genetic similarity (> 97% Hsp60 gene sequence identity). Several abundant species detected via amplicon sequencing (including *V. navarrensis* and *V. mimicus*) displayed site-specific ecotypes but remained uncultivated, highlighting methodological constraints in community characterisation. Our findings demonstrate how environmental heterogeneity drives fine-scale ecological differentiation in *Vibrio* populations, providing insights into mechanisms of bacterial adaptation in dynamic marine environments.

1 | Introduction

The genus *Vibrio* comprises diverse Gram-negative bacteria widely distributed in estuarine and coastal environments. These bacteria demonstrate remarkable adaptability through rapid growth, high environmental responsiveness, and distinctive morphological features including curved rod shapes and polar flagella that enhance their motility (Khan et al. 2010). Despite their relatively low proportional abundance (typically 1%–5% of bacterioplankton), *Vibrio* species are ecologically significant, with population densities often comparable to other major bacterial groups in coastal ecosystems, such as the *Roseobacteraceae* (Buchan et al. 2005). Their ecological significance extends beyond their relatively low abundance, as *Vibrio* species occupy diverse niches ranging from free-living bacterioplankton to symbionts of marine organisms, including corals, sponges, and commercially important shellfish (Nyholm and McFall-Ngai 2004; Yildiz and Visick 2009; Main et al. 2015; Greenfield et al. 2017).

Temperature emerges as a critical factor governing *Vibrio* population dynamics, as evidenced by clear seasonal patterns with peak

abundances during summer months when water temperatures exceed 20°C (Baker-Austin et al. 2013; Yung et al. 2015; Jesser and Noble 2018). Species-specific responses to temperature are notable: while *V. parahaemolyticus* maintains year-round presence, *V. vulnificus* and *V. cholerae* show predominantly summer occurrence (Whitesides and Oliver 1997). This seasonal variation is partly explained by their ability to enter a viable but non-culturable (VBNC) state—a survival strategy characterised by metabolic dormancy while maintaining cellular integrity and virulence potential (Pinto et al. 2015). During unfavourable conditions, *Vibrio* cells enter the VBNC state through morphological and physiological changes, later resuscitating when conditions improve (Xu et al. 1982). This adaptation, combined with their rapid growth rates under optimal conditions, enables Vibrio populations to respond swiftly to environmental changes (Baker-Austin et al. 2013; Yung et al. 2015).

Vibrio species exhibit remarkable functional diversity in marine ecosystems, from pathogenic relationships to biogeochemical cycling. As pathogens, *V. parahaemolyticus*, *V. vulnificus*, and *V. cholerae* pose significant public health concerns through waterborne and seafood-associated diseases, with infection rates increasing alongside rising ocean temperatures (Baker-Austin et al. 2013; Kokashvili et al. 2015; Garrido-Maestu et al. 2016). In tropical and subtropical regions, *Vibrio* infections account for a significant proportion of seafood-borne illnesses (Gao et al. 2022), with *V. parahaemolyticus* being the leading cause of seafood-associated gastroenteritis (McLaughlin et al. 2005; Ndraha et al. 2020). Additionally, species like *V. alginolyticus* and *V. coralliilyticus* threaten marine aquaculture, causing substantial economic impacts through diseases in farmed shrimp, fish, and molluscs (Gradoville et al. 2018; de Souza Valente and Wan 2021). Beyond pathogenicity, *Vibrio* species contribute significantly to marine nutrient cycling through their metabolic versatility, particularly in breaking down complex biopolymers like chitin, which they can utilise as both carbon and nitrogen sources (Meibom et al. 2004; Pruzzo et al. 2008; Sampaio et al. 2022).

Recent advances in molecular techniques, particularly 16S rRNA and Hsp60 amplicon sequencing, have enhanced our understanding of *Vibrio* ecology beyond the limitations of traditional culture-based methods (Hofer 2018; Jesser and Noble 2018). The Hsp60 gene, encoding a highly conserved heat shock protein, provides finer taxonomic resolution than the 16S rRNA gene for *Vibrio* species identification and has become an important tool for studying *Vibrio* diversity and evolution (Hunt et al. 2008; Yung et al. 2015). While this study focuses on molecular and culture-based approaches to investigate *Vibrio* community dynamics, it is important to acknowledge the growing role of genome-based taxonomy in *Vibrio* research. Whole-genome sequencing (Janecko et al. 2021; Brumfield et al. 2023) and multilocus sequence typing (MLST) (Sawabe et al. 2013) have been instrumental in delineating new species, refining genus boundaries, and identifying ecologically significant variants, which are increasingly recognised as critical for understanding *Vibrio* diversity and their ecological roles.

This study combines both molecular and culture-based approaches to investigate *Vibrio* community dynamics across two contrasting coastal environments in Hong Kong: Clear Water Bay (CWB), characterised by mesotrophic conditions and high salinity (> 30 ppt), and Deep Bay (DB), a eutrophic estuarine system with variable salinity (15–30 ppt). Through intensive sampling over a 1-year period (June 2020–June 2021), we analyse how *Vibrio* population structure responds to environmental heterogeneity by measuring key parameters including temperature, salinity, dissolved oxygen, chlorophyll-a, and nutrient concentrations. This comprehensive approach aims to elucidate the environmental drivers of *Vibrio* diversity and abundance, providing insights into their potential responses to climate change in tropical coastal systems.

2 | Materials and Methods

2.1 | Study Site and Sampling

Monthly seawater sampling was conducted from June 2020 to June 2021 at two coastal locations in Hong Kong: Deep Bay (DB) in the northwest and CWB Pier (CWB) in the east (Figure 1A). Surface water samples (15 L) were collected at 2 m depth. Environmental parameters were measured in situ using a YSI ProDSS Multiparameter Digital Water Quality Meter. Parameters included temperature, dissolved oxygen, salinity, pH, and turbidity. Nutrient analyses (ammonium, nitrites, nitrates, silicates, orthophosphate, and total phosphorus) were performed in triplicate according to APHA standard methods (detailed protocols in Table S1). For chlorophyll analysis, duplicate 25 mL seawater samples were filtered through 0.22 μm polycarbonate membranes (Whatman) and stored at −80°C until processing.

2.2 | DNA Extraction

Microbial biomass from 500 mL seawater samples was collected on 0.22 μm Supor-200 membrane filters (Pall Corporation) and flash-frozen in liquid nitrogen. DNA was extracted using a modified DNeasy Plant Minikit protocol (Qiagen). Modifications included: (i) mechanical lysis using a mixture of 0.1 and 0.5 mm glass beads with 2-min bead beating, (ii) three freeze–thaw cycles alternating between 65°C and liquid nitrogen in Buffer AP1, (iii) Proteinase K digestion (45 μL, 55°C, 1 h), and (iv) RNase A treatment (4 μL, 65°C, 10 min). DNA quality and concentration were determined using a Biodrop spectrophotometer prior to storage at −80°C.

2.3 | Quantitative PCR Analysis

The abundance of total *Vibrio* bacteria and bacterial community was assessed using quantitative PCR (qPCR) with SYBR Green detection on the CFX96 Touch Real-Time PCR Detection System (Bio-Rad, USA). For *Vibrio*-specific amplification, the 16S rRNA gene oligonucleotide primers V567F and V680R were employed (Thompson et al. 2004), while primers B967F and B1046R were used to quantify total bacterial abundance (Sogin et al. 2006). Standard curves were generated using synthetic 16S rRNA gene fragments following established protocols (Han et al. 2023). All reactions were performed in triplicate, including negative controls. The amplification efficiency for all assays ranged between 95% and 105% with R^2 values exceeding 0.99, confirming the reliability of the quantification.

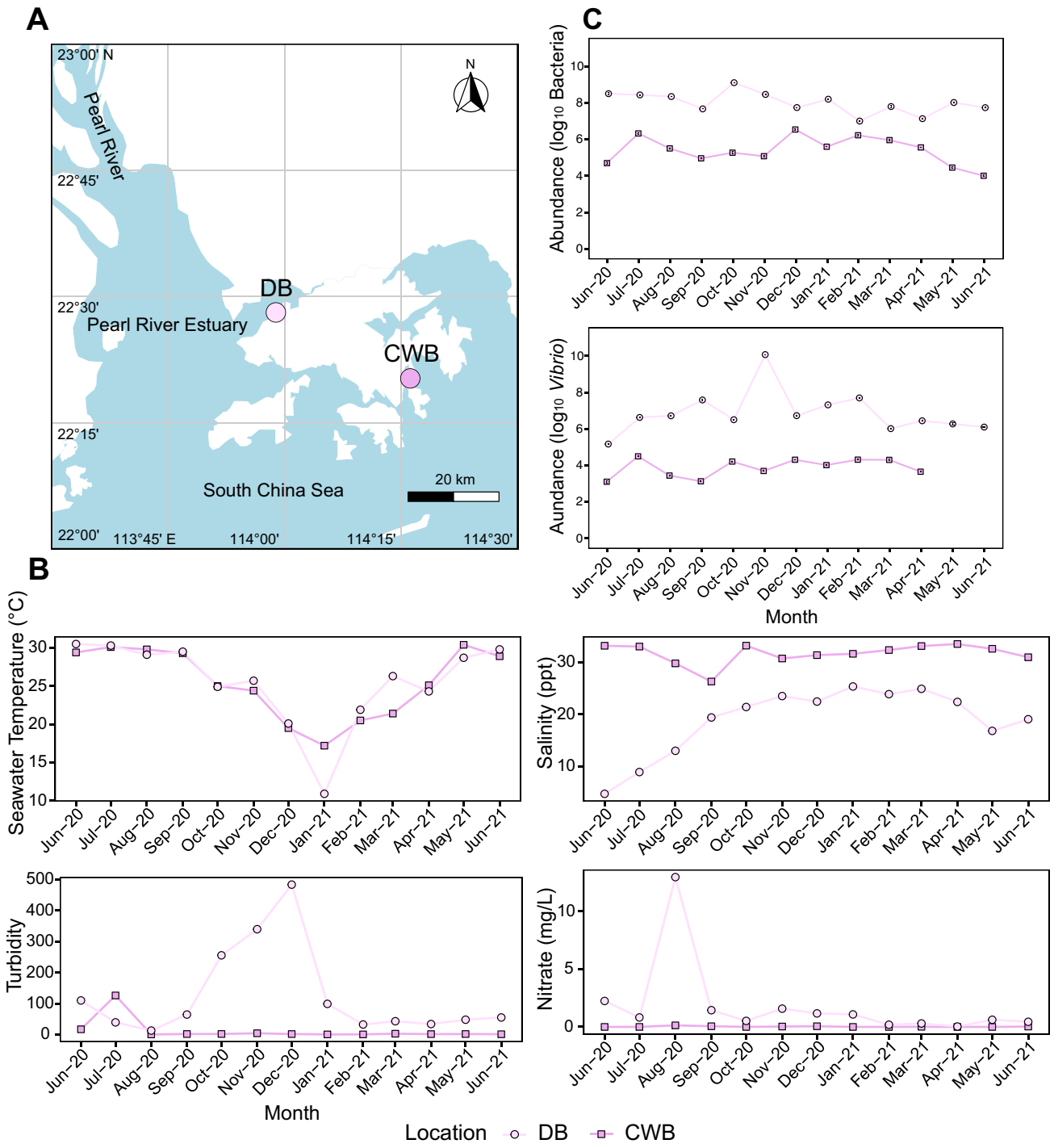

FIGURE 1 | Sample locations and environmental parameters in the Pearl River Estuary over a 1-year monitoring period (June 2020–June 2021) (A) Map of the Pearl River Estuary in South China showing the two sampling stations: Deep Bay (DB) and Clear Water Bay (CWB). (B) Seasonal variation of physicochemical parameters at both sampling sites, including temperature (°C), salinity (ppt), nitrate (mg/L), pH, dissolved oxygen (mg/L), and turbidity. (C) Temporal dynamics of microbial abundance over the sampling period, showing $\log_{10}$-transformed counts of total bacteria and *Vibrio* spp. at both sampling locations.

2.4 | Amplicon Library Preparation and Sequencing

Bacterial community composition was analysed using two marker genes: 16S rRNA and Hsp60 gene. The V4-V5 region of the 16S rRNA gene was amplified using barcoded universal primers 515F-Y and 926R (Parada et al. 2016), while the Hsp60 gene was amplified using barcoded primers Vib-hspF3-23 and Vib-hspR401-422 (King et al. 2019) (Table S2). PCR reactions (50 μL) contained NEBNext Ultra II Q5 Master Mix (25 μL), forward and reverse primers (2 μL each, 10 μM), DNA template (2 μL), and PCR-grade water. The 16S rRNA gene amplification

consisted of initial denaturation (98°C, 3 min), 30 cycles of denaturation (98°C, 45 s), annealing (50°C, 60 s), and extension (72°C, 90 s), followed by final extension (72°C, 10 min). The Hsp60 gene amplification protocol included initial denaturation (98°C, 2 min), 30 cycles of denaturation (98°C, 30 s), annealing (50°C, 30 s), and extension (72°C, 30 s), with final extension (72°C, 10 min). Amplicon libraries were sequenced using Novaseq PE250 (Novogene, China).

2.5 | Sequence Data Processing

Raw sequence data from both markers underwent quality control and processing using standardised bioinformatic pipelines. For 16S rRNA gene sequences, quality trimming was performed using Sickle (Q25 threshold, 10 nt window) (Joshi and Fass 2011), followed by merging and quality-filtering of paired-end reads using USEARCH v11.0.667 (≥95% identity, ≥20 nt overlap, ≥200 nt length, maximum expected error <0.005) (Edgar 2013). Primer sequences were removed using Cutadapt v3.7 (Martin 2011). After filtering Illumina artefacts and sequences with ambiguous bases, 2,875,894 reads were retained and processed into amplicon sequence variants (ASVs) through dereplication and denoising using UNOISE3 (Edgar and Flyvbjerg 2015). Taxonomic assignment using Qiime2 with the SILVA 138 SSU database (0.8 confidence threshold) (Quast et al. 2013; Bolyen et al. 2019) yielded 4830 ASVs after removing chloroplast, mitochondrial, and eukaryotic sequences. The Hsp60 gene sequences underwent similar processing, with modified primer trimming parameters in Cutadapt v3.7 (zero errors for forward primer, maximum two errors for reverse primer) (Martin 2011), resulting in 3,617,372 quality-filtered reads that were processed into ASVs and taxonomically classified using BLAST searches against GenBank through Geneious Prime software (Kearse et al. 2012). After removing eukaryotic and viral sequences, 13,285 ASVs remained.

2.6 | Bacterial Community Analysis

Bacterial and *Vibrio* community compositions were analysed using Bray–Curtis dissimilarity matrices and visualised through non-metric multidimensional scaling (NMDS) with 95% confidence ellipses using R packages 'vegan' (Dixon 2003) and 'ggplot2' (Wickham 2011). Analysis of similarities (ANOSIM) tested for community differences between sites and seasons. Environmental drivers of community variation were identified through stepwise selection ('ordistep' function) and analysed using Canonical Correspondence Analysis (CCA), with individual variable significance assessed through marginal effects. For *Vibrio*-specific analysis, ASVs were grouped by species and the top 10% most abundant ASVs were correlated with environmental parameters using Pearson coefficients ('corrplot' package). These dominant ASVs were aligned using MUSCLE (Edgar 2004), trimmed with trimAl (gap threshold 0.5) (Capella-Gutiérrez et al. 2009), and used to construct a maximum likelihood phylogenetic tree. ASV distribution patterns across samples were visualised using heatmaps, and correlations between the top ~5% abundant species from each location and environmental factors were determined using Pearson's correlation coefficients.

2.7 | *Vibrio* Strain Isolation and Characterisation

Vibrio strains were isolated from size-fractionated seawater samples (>50 μm, 50–5 μm, 5–1 μm, and 1–0.22 μm) collected monthly at both study sites following Hunt et al. (2008). Samples were plated on TCBS Agar (1% NaCl) and incubated at room temperature for 18–24 h. Colonies were purified through three alternating streaks on LB Agar (2% NaCl) and TCBS Agar (Thompson et al. 2004), then stored in 20% glycerol at −80°C after growth in LB broth (20 g L −1 NaCl). DNA was extracted by heat treatment (98°C, 10 min). Isolates were characterised by Hsp60 gene sequencing using degenerate primers H279 and H280 (Goh et al. 1996). PCR reactions (25 μL) contained 0.2 mM dNTPs, 3.75 mM MgCl2, 0.5 μM each primer, 1X PCR buffer, 0.75 U Taq DNA polymerase (Takara), and DNA template. Amplification consisted of initial denaturation (94°C, 3 min), 30 cycles of denaturation (94°C, 1 min), annealing (37°C, 1 min), and extension (72°C, 1 min), followed by final extension (72°C, 10 min). PCR products (~600 bp) were verified by gel electrophoresis, purified using PureLink Quick Gel Extraction Kit (Invitrogen), and sequenced at TechDragon Limited (Hong Kong).

2.8 | Phylogenetic Analysis

Vibrio isolate Hsp60 gene sequences were processed in Geneious Prime 2021.1.1 (Kearse et al. 2012), including trimming, manual quality checks, and de novo assembly into 400–600 bp consensus sequences. Multiple sequence alignment was performed using MAFFT (Katoh et al. 2005), followed by the removal of poorly aligned regions using trimAl (gap threshold 0.5) (Capella-Gutiérrez et al. 2009). A Maximum Likelihood tree was constructed using IQTree (Minh et al. 2020) employing the LG + F + R4, and visualised with isolation temperatures in Interactive Tree of Life (iTOL) (Letunic and Bork 2021). Isolates were partitioned into ecologically cohesive clades according to genetic and ecological similarity using AdaptML (Hunt et al. 2008) and visualised using the Interactive Tree of Life tool (Letunic and Bork 2021). For comparison of culture-dependent and culture-independent methods, Hsp60 gene sequences from ASVs and isolates were trimmed to the same gene region and analysed using identical phylogenetic methods. Species identification was conducted using NCBI BLAST.

2.9 | Growth Rate Determination

Vibrio strains with high Hsp60 gene sequence similarity but isolated from different water temperatures were selected for thermal growth characterisation. Overnight precultures grown in LB medium at room temperature were used to inoculate fresh LB medium in 96-well plates (100 μL/well). Growth curves were generated by monitoring optical density (600 nm) using a CLARIOstar Plus microplate reader (BMG Labtech) across a

temperature gradient from 8° to 52°C at 4°C intervals until cultures reached stationary phase.

3 | Results and Discussion

3.1 | Distinct Physicochemical Characteristics of Coastal and Estuarine Sampling Sites

The comparative environmental analysis revealed distinct physicochemical profiles between Clear Water Bay (CWB, coastal water) and Deep Bay (DB, estuarine water near the Pearl River mouth) (Figures 1B and S1). CWB exhibited stable marine conditions with typical salinity (26.33‰–33.57‰), while DB demonstrated variable, lower salinity (4.67‰–25.38‰), consistent with previous Pearl River Estuary studies (Harrison et al. 2008). Although temperature patterns were similar between sites, their environmental characteristics differed markedly in other parameters. DB showed elevated turbidity (32.58–483.44 NTU) and nutrient concentrations (NH_4: 0.18–1.42 mg/L, TP: 0.12–1.01 mg/L) due to riverine inputs (Yin et al. 2004), resulting in higher chlorophyll a levels characteristic of nutrient-enriched estuaries (Paerl et al. 2006). The site also showed fluctuating pH values (7.41–8.33), reflecting variable riverine influences (Duarte et al. 2013). In contrast, CWB maintained lower turbidity (0.58–126.23 NTU), reduced nutrient levels (NH_4;: 0–0.02 mg/L, TP: 0–0.52 mg/L) typical of coastal waters (Cloern et al. 2014), and more stable pH conditions (7.86–8.35). These environmental distinctions likely drive the development of site-specific microbial communities: DB's dynamic, nutrient-rich conditions potentially supporting a diverse microbiome adapted to rapid physicochemical fluctuations, while CWB's stable, oligotrophic environment possibly harbours a more specialised microbial community adapted to consistent marine conditions.

3.2 | Site-Specific Variation in Bacterial and *Vibrio* Abundances

Quantitative PCR analysis revealed striking differences in microbial population dynamics between the two sites (Figure 1C). The oligotrophic CWB maintained relatively modest microbial populations (bacterial abundances: 1.03×10^4 to 3.54×10^6 copies/mL; *Vibrio*: below detection limit to 3.17×10^4 copies/mL), consistent with observations in other oligotrophic coastal waters (Shi et al. 2018; Wang et al. 2020). In contrast, the nutrient-enriched DB exhibited substantially higher and more variable densities (bacterial counts: 1.02×10^7 to 1.30×10^9 copies/mL; *Vibrio*: 1.49×10^5 to 5.04×10^7 copies/mL), aligning with patterns observed in nutrient-rich estuarine systems (Zhou et al. 2017; Gradoville et al. 2018). This pronounced disparity in population sizes, spanning several orders of magnitude, reflects the influence of environmental conditions, particularly the Pearl River's nutrient-rich freshwater inputs at DB, in shaping microbial community structures (Wang et al. 2020). The observed *Vibrio* abundance patterns parallel findings from both the South China region (Xu et al. 2020) and other major estuarine systems (Baker-Austin et al. 2013), where *Vibrio* populations typically increase with temperature and nutrient availability.

3.3 | Spatial and Temporal Differences in Bacterial Community Composition and Their Environmental Drivers

Canonical Correspondence Analysis (CCA) revealed that community patterns correlated with environmental variability, which was markedly greater at DB where annual temperature and salinity fluctuations (19.6°C and 20.71‰) substantially exceeded those at CWB (13.2°C and 7.24‰). While DB exhibited pronounced seasonal community differences, CWB maintained a relatively stable community composition throughout the year (Figure 2A), consistent with observations of community stability in constant marine environments (Fuhrman et al. 2015).

Forward selection identified multiple significant drivers of community structure ($p < 0.001$), with salinity emerging as the primary factor (marginal effects of terms, $p = 0.001$) (Figure 2A). This reflects the distinct geographic characteristics of the sampling locations: DB, influenced by the Pearl River, experiences significant seasonal changes with 80% of annual discharge occurring in summer, leading to pronounced salinity fluctuations and elevated nutrient levels typical of estuarine systems (Xu et al. 2010). In contrast, CWB maintains stable, oligotrophic oceanic conditions with minimal river influence and consistent salinity, characteristic of marine environments in Hong Kong's eastern waters (Zong et al. 2010). The community shifts observed along this salinity gradient align with patterns reported in similar estuarine–marine transitions worldwide (Tee et al. 2021).

Temperature was another significant factor (marginal effects of terms, $p = 0.002$) (Figure 2A), showing primarily seasonal effects. Both sites displaying similar monthly patterns except during winter extremes (CWB: 17.2°C, DB: 10.9°C; Figure 1B). Historical data (2010–2020) from the Marine Water Quality Monitoring Program confirmed these long-term environmental differences, with Deep Bay Station DM3 showing annual salinity variations of 19.5‰ compared to Port Shelter Station PM7's 6.5‰ (Figure S2). These findings parallel previous demonstrations of how riverine inputs significantly alter estuarine microbial dynamics through salinity fluctuations (Crump et al. 2004). The enhanced environmental variability at DB corresponded with significantly higher microbial diversity (Shannon index, Wilcoxon Signed-Rank Test, $p = 0.04$) (Figure S3), aligning with previous observations of how seasonal fluctuations shape microbial community structure in coastal and estuarine ecosystems (Gilbert et al. 2012; Ward et al. 2017; Wang et al. 2021).

We assessed multicollinearity among environmental predictors using Variance Inflation Factors (VIFs). The analysis revealed varying degrees of interdependence among environmental variables (Salinity: 1.89; Turbidity: 3.50; NH_4: 4.51; Temperature: 1.23; Chlorophyll: 1.16). While all VIFs remained below the critical threshold of 5, NH_4 exhibited moderate multicollinearity (4.51), likely reflecting its relationship with river discharge patterns that also influence turbidity (3.50). Temperature and salinity, the two most significant drivers, showed low VIF values, confirming their independent influences on community structure rather than being

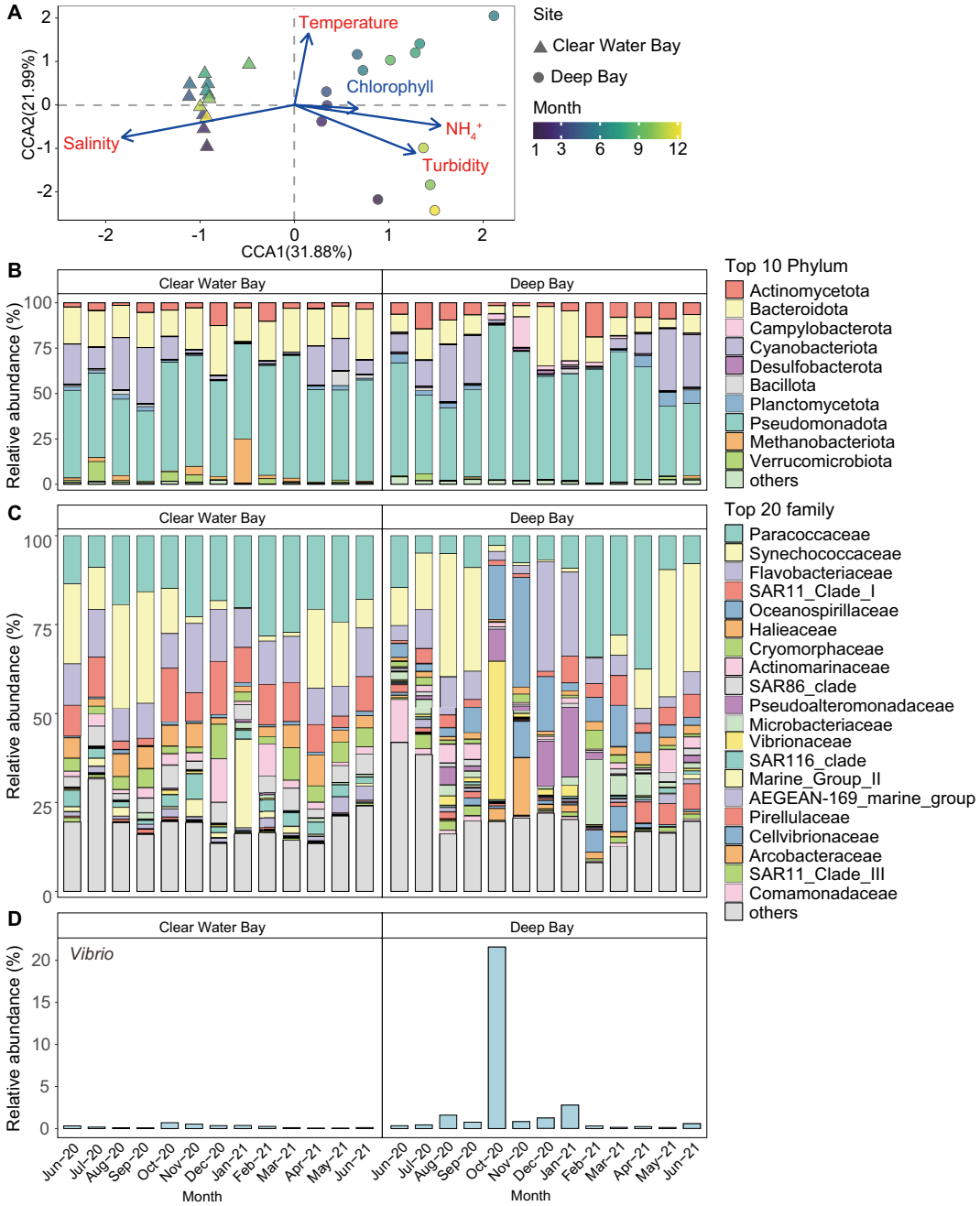

FIGURE 2 | Microbial community composition and environmental drivers based on 16S rRNA amplicon sequencing. (A) Canonical correspondence analysis (CCA) showing microbial community distribution in relation to environmental variables. Red highlighted text represents significant environmental drivers ($p < 0.05$) through marginal effects testing. (B) Monthly relative abundance of top 10 bacterial phyla in DB and CWB. (C) Monthly relative abundance of top 20 bacterial families in DB and CWB. (D) Monthly relative abundance of *Vibrio* populations in CWB and DB.

confounded variables. These results strengthen our interpretation that temperature and salinity independently drive community structure across the contrasting environments of DB and CWB.

3.4 | Seasonal Dynamics in Total Bacterial Communities

Analysis of 16S rRNA gene sequences identified Pseudomonadota (54.7%), Bacteroidota (17.0%), and Cyanobacteriota (12.5%) as the dominant phyla across both sites (Figure 2B), reflecting typical marine bacterioplankton assemblages driven by their diverse metabolic capabilities (Sunagawa et al. 2015; Ward et al. 2017). Despite these similarities, several key taxa showed distinct spatial and temporal distribution patterns. The archaeal phylum Methanobacteriota showed distinct spatial variation, reaching 24.2% abundance in CWB (January 2021) while remaining below 1% in DB, suggesting niche-specific adaptations to local organic matter and water chemistry gradients. Cyanobacterial abundances displayed clear seasonal cycles driven by temperature and light availability (Paerl et al. 2011; Xu et al. 2024), with summer

peaks (CWB: 7%–30%; DB: 9%–34%) that declined to winter lows (CWB: < 3%; DB: < 6%).

At the family level, *Paracoccaceae* (16.1%), *Synechococcaceae* (12.5%), and *Flavobacteriaceae* (10.3%) dominated both communities but followed distinct seasonal patterns (Figure 2C). While *Cyanobciaceae* showed expected summer peaks corresponding to increased temperature and solar radiation, *Rhodobacteraceae* and *Flavobacteriaceae* showed winter dominance. This seasonal pattern contrasts with their typical spring–summer peaks in temperate waters (Gilbert et al. 2012; Bunse and Pinhassi 2017), but aligns with subtropical winter characteristics: moderate temperatures combined with enhanced vertical mixing increase nutrient availability (Xu et al. 2024) and winter monsoons further amplify this effect by introducing nutrient-rich waters (Needham and Fuhrman 2016). These conditions favour heterotrophic bacteria like *Paracoccaceae* and *Flavobacteriaceae*, which excel at utilising dissolved organic matter through diverse metabolic pathways (Teeling et al. 2016; Francis et al. 2019).

DB additionally experienced episodic blooms of typically rare bacterial families, including *Vibrionaceae* (37.0%, October), *Oceanospirillaceae* (29.9%), and *Arcobacteraceae* (15.6%, November) (Figure 2C). These blooms align with previous studies where *Vibrionaceae* proliferated during periods of high dissolved organic carbon and phosphate in estuarine waters (Orsi et al. 2016; Liang et al. 2019). These opportunistic taxa possess specialised metabolic strategies that enable rapid response to transient nutrient pulses: *Oceanospirillaceae* exploit nitrate influxes through dissimilatory nitrate reduction to ammonium (Avendaño et al. 2024), while *Arcobacteraceae* couple sulfur oxidation with nitrate reduction in nutrient-enriched, micro-anoxic zones (Callbeck et al. 2019).

3.5 | *Vibrio* Community Composition

Initial analysis of *Vibrio* communities through 16S rRNA gene ASV filtering revealed significant differences between sampling sites, with consistently higher relative abundances in DB compared to CWB (Wilcoxon signed-rank test, $p = 0.01$) (Figure 2D). While *Vibrio* typically constituted approximately 1% of the bacterial community, a notable bloom event in DB during October 2020 reached 21.6% relative abundance. However, 16S rRNA gene analysis provided limited taxonomic resolution, successfully differentiating only *V. xiamenensis* (representing < 1% of total *Vibrio* population) due to high sequence similarity among *Vibrio* species (Links et al. 2012).

To achieve finer taxonomic resolution, we employed partial Hsp60 gene sequence (~487 bp) analysis (Jesser and Noble 2018), which revealed substantially greater diversity within coastal *Vibrio* communities. This approach identified 1001 *Vibrio* ASVs categorised into 37 distinct species and 202 environmental clones. The environmental clone group, comprising 444 different ASVs, demonstrated remarkable diversity that would have remained undetected using 16S rRNA gene sequencing alone. The superior resolution of Hsp60 gene sequences in distinguishing closely related bacterial species made it our preferred method for subsequent community analyses.

3.6 | Spatiotemporal Distribution of Major Pathogenic *Vibrio* Species

The *Vibrio* community exhibited complex spatiotemporal patterns, with most species individually comprising less than 10% of the total population (Figure 3A). Major human pathogens showed consistent presence throughout the study period but with distinct spatial and seasonal preferences. *V. cholerae* in CWB maintained predominantly low levels (< 7%) except for an unusual winter bloom (23.2%, January 2021), contrasting with documented summer peaks typically observed in tropical regions (Vezzulli et al. 2016). In DB, both *V. parahaemolyticus* and *V. vulnificus* showed higher abundance (up to 26.2% and 20.7%, respectively), consistent with their preference for nutrient-rich coastal waters (Johnson et al. 2010). These two DB-dominant pathogens exhibited distinct seasonal patterns. *V. parahaemolyticus* displayed bimodal peaks during late summer 2020 (26.2%, 16.4%) and early spring 2021 (11.5%, 18.1%), following temperature-driven patterns observed globally (Martinez-Urtaza et al. 2010). *V. vulnificus* demonstrated clear summer prevalence, with peaks in June–September (up to 20.7%), aligning with temperature-dependent patterns (> 20°C) reported in oyster-growing regions worldwide (Motes et al. 1998). Their elevated presence in DB, an active oyster farming area, raises concerns about shellfish safety under projected climate change scenarios (Baker-Austin et al. 2013).

Beyond these well-known pathogens, emerging *Vibrio* species also displayed distinct temporal dynamics. *V. mimicus* in DB exhibited pronounced summer dominance with peak abundances of 47.1%–38.6% (June–July 2020) and 70.6%–26.1% (May–June 2021), dropping below 4% in winter. This species serves as a reservoir of virulence genes in marine environments (Guardiola-Avila et al. 2016), making its significant presence noteworthy. In contrast, *V. navarrensis* maintained consistently high abundance (> 10%) at both sites during October–December 2020 and May–June 2021 in CWB, and June–November 2020 and April 2021 in DB. Originally isolated from sewage, its widespread presence suggests adaptation to diverse environments (Gladney and Tarr 2020).

Location specificity was particularly evident among several other *Vibrio* species, reflecting specialised ecological niches. DB exclusively harboured *V. breoganii, V. maritimus*, and *V. panuliri*, while *V. paracholerae* and *V. rarus* were restricted to CWB. These distinct spatial distributions align with documented ecological preferences. *V. breoganii* is strongly associated with macroalgal substrates (Corzett et al. 2018), *V. maritimus* forms mutualistic relationships with diatoms (Zhu et al. 2022), and *V. panuliri* and *V. rarus* demonstrate host specificity with marine animals including lobster, abalone, and coral (Sawabe et al. 2007; Kumari et al. 2014; Rubio-Portillo et al. 2014). The restriction of certain species to CWB likely relates to its higher salinity and lower nutrient levels typical of oceanic waters. These habitat-specific distributions reflect the complex interplay between *Vibrio* species and their environmental niches, supporting previous findings on niche partitioning in coastal *Vibrio* communities (Hunt et al. 2008).

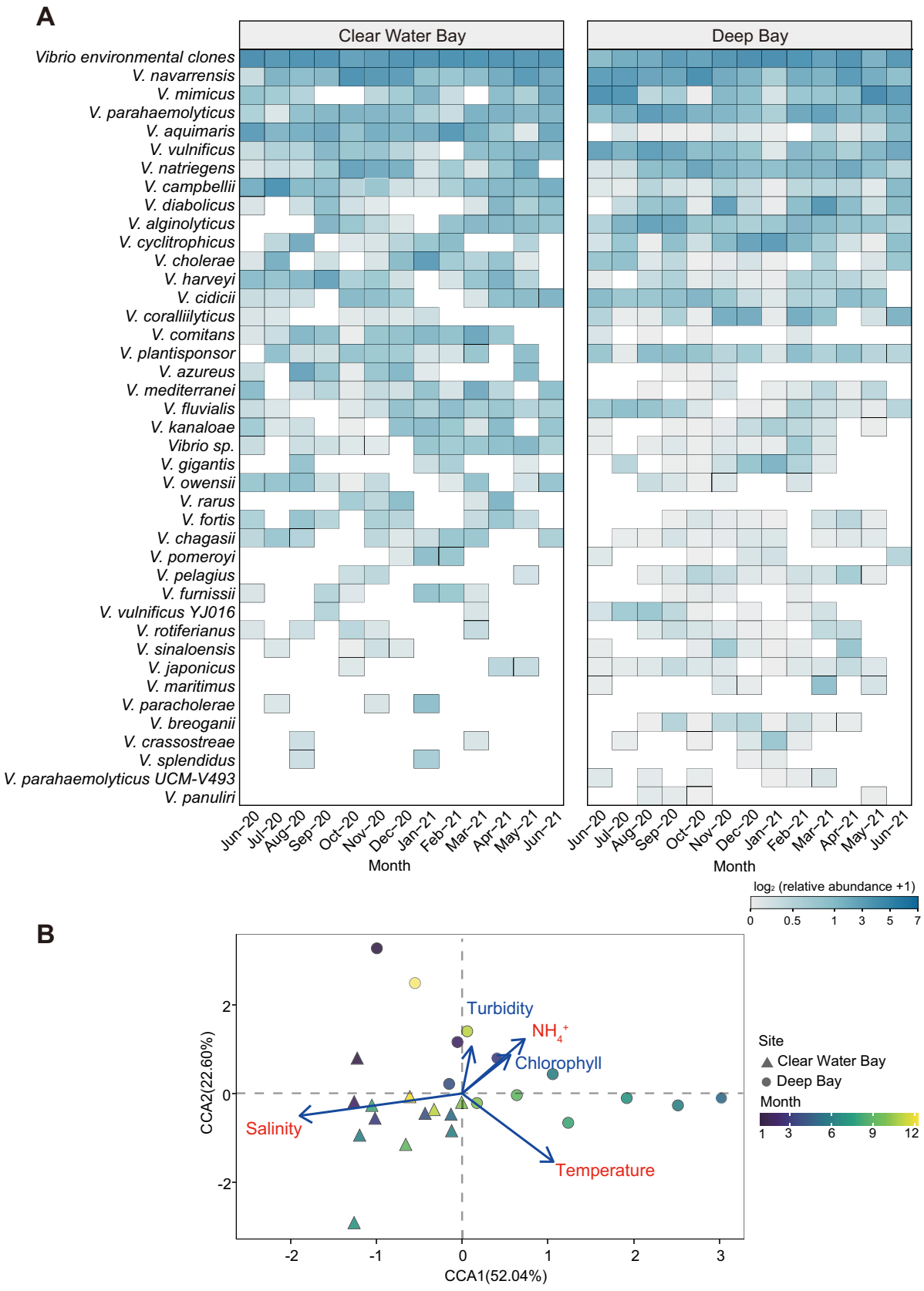

FIGURE 3 | Temporal and spatial dynamics of *Vibrio* species in coastal waters. (A) Heatmap showing monthly relative abundance ($\log_2$-transformed) of *Vibrio* species in CWB and DB. Colour intensity indicates abundance levels, with darker colours representing higher relative abundance. *Vibrio* species are arranged from highest to lowest overall abundance. (B) Canonical Correspondence Analysis (CCA) of *Vibrio* community composition in relation to environmental variables. Red highlighted text represents significant environmental drivers ($p < 0.05$) through marginal effects testing.

3.7 | Distinct Community Composition and Seasonal Dynamics of *Vibrio* Species

The *Vibrio* communities in DB and CWB exhibited marked differences in composition, dominance patterns, and community structure. only ASV-level analysis revealed location-specific distributions, with only 22 of the top 50 abundant ASVs (representing ~5% of total abundance) shared between sites, primarily belonging to *V. navarrensis* and *V. natriegens*. Community evenness analysis demonstrated significantly higher Pielou's evenness in CWB compared to DB (Wilcoxon signed-rank test, $p < 0.01$) (Figure S3), indicating more balanced communities in CWB versus oligarchic assemblages in DB. The estuarine DB site was characterised by pronounced dominance of several species: *V. diabolicus* (max 34.0%), *V. mimicus* (max 45.9%), *V. navarrensis* cluster (max 44.6%), *V. cyclitrophicus*-like cluster (max 29.9%), and *V. coralliilyticus*-like cluster (max 19.4%). The high abundance of known oyster pathogens (*V. mimicus*, *V. crassostreae*, *V. cyclitrophicus*) corresponds with local oyster farming activities (Bruto et al. 2017). In contrast, the oceanic CWB site typically maintained lower relative abundances for most species (< 15%), with exceptions during bloom events of *V. campbellii* (42.1%, July 2020), *V. navarrensis* (40.4%, October 2020), and *V. cholerae* (23.0%, January 2021), which coincided with significant decreases in community evenness (Figure S4).

Distinct seasonal succession patterns emerged at each site, reflecting *Vibrio*'s ability to respond to specific environmental triggers (Ceccarelli and Colwell 2014). In CWB, *V. campbellii* cluster dominated during summer months (June–September 2020, March–June 2021), while *V. navarrensis* and *V. natriegens* peaked in winter (October–December 2020), and *V. cholerae* showed winter dominance (December 2020–January 2021) (Figure 3A). *V. aquimaris* and *V. navarrensis* demonstrated year-round presence, suggesting broader environmental tolerance. DB showed stronger seasonal patterns with *V. mimicus* dominating in summer (> 45.9% in June–July 2020, May–June 2021) and *V. vulnificus* showing summer-specific presence (June–August 2020). Winter dominance in DB shifted to *V. diabolicus*, *V. crassostreae*-like, *V. cyclitrophicus*-like, and *V. coralliilyticus*-like clusters. While these patterns reflect DNA-based detection, our metabarcoding approach cannot distinguish between active cells and those in the viable but non-culturable (VBNC) state, which *Vibrio* species often enter during unfavourable conditions (Whitesides and Oliver 1997).

Phylogenetic analysis revealed ecological differentiation through distinct *V. mimicus* ecotypes between the two locations (Figure 4). Despite its presence at both sites, *V. mimicus* strains dominating DB formed a clade more closely related to *V. diabolicus*, while those from CWB clustered with *V. cholerae*. This phylogenetic divergence suggests niche-specific adaptation of *V. mimicus* populations to contrasting environments with different ecological pressures. The ability of Hsp60 gene sequences to resolve such fine-scale population structure demonstrates its value for understanding ecological differentiation among closely related strains. This observation contributes to growing evidence that seemingly identical *Vibrio* species can comprise distinct ecotypes adapted to specific environmental conditions, challenging traditional species-level understanding of *Vibrio* ecology and evolution (Shapiro et al. 2012; Yung et al. 2015).

3.8 | Environmental Drivers Shaping *Vibrio* Dynamics: From Species to Community Level

Pearson correlation analysis revealed specific relationships between environmental parameters and *Vibrio* species abundance patterns, providing valuable insights into their ecological preferences. *V. mimicus* and *V. vulnificus* ASVs, which dominated summer communities in DB, showed moderate to strong negative correlations with salinity (Figure 4), aligning with their documented preference for low-salinity conditions (Chowdhury et al. 1989; Matteucci et al. 2015). *V. vulnificus* additionally exhibited positive correlations with nutrient concentrations (phosphorus, nitrates, and silicates), highlighting its potential as a bioindicator for nutrient-enriched waters from terrestrial runoff or anthropogenic inputs (Westrich et al. 2016; Kopprio et al. 2020). The *V. cyclitrophicus*-like cluster, prevalent during winter months in DB, demonstrated a negative correlation with temperature, while *V. coralliilyticus*-like strains showed positive correlations with ammonium, turbidity, and chlorophyll levels, suggesting potential associations with phytoplankton dynamics or post-bloom conditions.

Our comprehensive analysis of all 78 *Vibrio* ASVs unveiled the intricate nature of environmental influences on *Vibrio* populations. While specific species showed clear environmental preferences, less than half of ASVs displayed statistically significant correlations with environmental variables ($p < 0.05$) (Figure 4). These moderate correlations (Pearson's $r < 0.5$) suggest that *Vibrio* ecology is shaped not only by abiotic factors but also by unmeasured variables and biotic interactions. For instance, dissolved organic carbon (DOC) and particulate organic matter (POM)—key drivers of microbial growth—were not quantified in this study but likely influence *Vibrio* dynamics through substrate availability and biofilm formation (Takemura et al. 2014). Beyond abiotic factors, *Vibrio* species engage in diverse biological relationships, including beneficial associations with plankton (Erken et al. 2015), dynamic interactions with bacteriophages (Kalatzis et al. 2016; Yang et al. 2020), and complex ecological relationships with marine invertebrates and fish (Thompson et al. 2003). Future research should explore these additional factors that could enhance our understanding of how microbial competition, nutrient availability, and organic matter cycling interact to influence *Vibrio* dynamics.

Canonical Correspondence Analysis (CCA) of the entire *Vibrio* community revealed a hierarchical organisation of environmental influences on *Vibrio* ecology. Temperature emerged as the primary driver of community composition, with both temperature ($p = 0.002$) and salinity ($p = 0.001$) showing statistical significance based on marginal effects analysis (Figure 3C). Multicollinearity among environmental predictors was assessed using Variance Inflation Factors (VIFs). The VIF values (Salinity: 1.56; Turbidity: 1.71; NH4: 1.97; Temperature: 1.50; Chlorophyll: 1.12) were all well below the threshold of 3, indicating minimal correlation among the environmental variables. These low VIF values confirm that each parameter contributes unique explanatory power to the model, strengthening the reliability of the identified temperature and salinity effects on the *Vibrio* community. This finding bridges the gap between species-specific responses and community-level patterns, demonstrating how broad physicochemical parameters

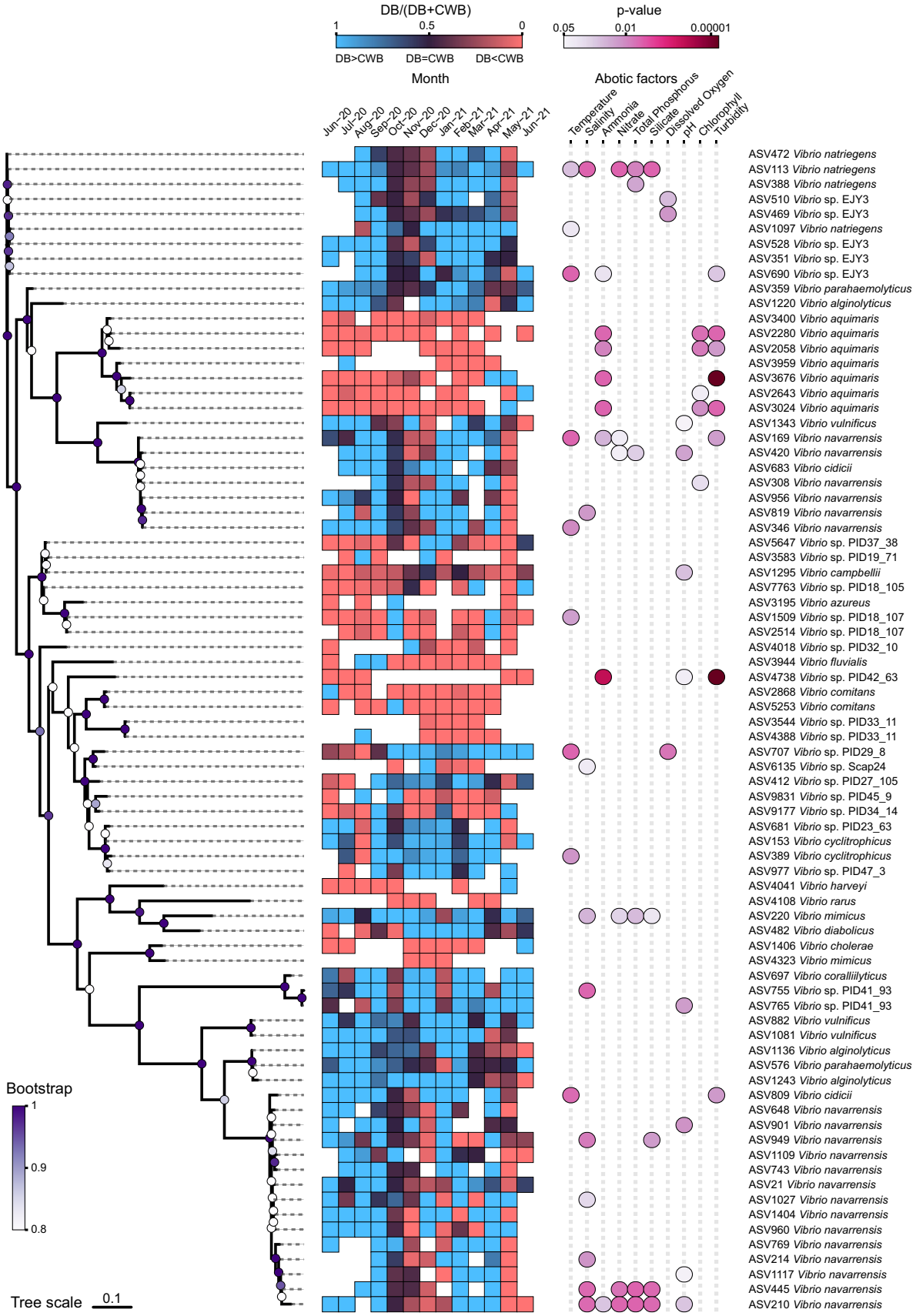

FIGURE 4 | Legend on next page.

FIGURE 4 | Phylogenetic distribution, site preference, and environmental correlations of Vibrio ASVs. The figure presents 79 Vibrio ASVs (amplicon sequence variants) identified across two sampling sites (DB and CWB) during a year-long monitoring period (June 2020–June 2021). Left panel: Phylogenetic tree with bootstrap values indicated by coloured circles at key nodes (tree scale: 0.1). Middle panel: Site preference for each ASV expressed as the ratio DB/(DB + CWB), where values approaching 1 (red) indicate DB dominance, 0.5 (white) indicate equal distribution, and 0 (blue) indicate CWB dominance. Statistical significance is denoted by circle size according to *p*-value thresholds. Right panel: Pearson correlation analysis between ASVs and ten environmental parameters, with red/blue indicating positive/negative correlations (circle size represents significance level).

orchestrate overall community structure while allowing for species-specific adaptations through biological interactions. This hierarchical organisation provides a framework for understanding how *Vibrio* communities maintain both stability and adaptability in response to environmental changes, offering valuable insights for predicting community responses to environmental variations in coastal ecosystems.

3.9 | Population Structure and Environmental Adaptation Patterns

Our culture-independent studies consistently demonstrated distinct bacterial and Vibrio communities between CWB and DB, prompting a detailed investigation into strain-level diversity through culturing methods. From June 2020 to June 2021, We successfully isolated 1521 Vibrio strains (828 from CWB, 693 from DB) over the 1-year sampling period, providing a robust foundation for examining fine-scale population structure and environmental adaptation patterns. To quantitatively assess environmental specialisation patterns, we employed AdaptML analysis on a Maximum Likelihood phylogenetic tree constructed from partial Hsp60 gene sequences. This approach identified statistically supported ecological habitats without making a priori assumptions about environmental or phylogenetic boundaries. After assigning isolate sequences to discrete environmental bins (5°C temperature intervals from < 15.1° to > 30°C and 5‰ salinity intervals from < 10.1‰ to > 30‰) based on isolation conditions, the AdaptML algorithm robustly identified three distinct habitats (H_A, H_B, and H_C) corresponding to different combinations of temperature and salinity preferences ($p < 0.0001$), revealing complex patterns of environmental specialisation across the *Vibrio* phylogeny (Figure 5).

3.10 | Temperature and Salinity Shape Distinct *Vibrio* Ecological Strategies

The primary division between CWB and DB populations appears driven by salinity preferences. Habitat H_A, predominantly comprising CWB strains (clades C1-C6) (Figure 5B), exhibited adaptation to higher salinity conditions (mostly > 25‰) (Figure 5C). This stenohaline adaptation distinguishes H_A from other habitats, as these clades showed similar temperature distributions to H_B strains but restricted salinity ranges. This suggests H_A strains may lack physiological mechanisms necessary for adapting to lower salinity, constraining their distribution to marine environments despite their broad temperature tolerance. In contrast, Habitat H_B, mainly represented by DB strains (clades C7-C10) (Figure 5B), thrived in moderate to lower salinity conditions (10.1‰–20‰) (Figure 5C). While sharing similar temperature ranges with H_A strains, these populations exhibited greater euryhalinity, enabling them to persist in the variable salinity conditions typical of estuarine environments.

Habitat H_C (clades C11-C13) revealed a distinct ecological strategy characterised by strong association with cooler temperatures (< 20°C), while maintaining broad tolerance across the salinity gradient (10.1‰–30‰) (Figure 5C). This temperature-specialised but salinity-generalist strategy indicates specialised winter populations that can persist across both marine and estuarine conditions. The clear temporal separation of these strains suggests temperature acts as the primary selective force structuring these populations, while their broad salinity tolerance enables them to occupy diverse coastal environments during cooler seasons.

3.11 | Thermal Adaptation Mechanisms and Physiological Trade-Offs

To understand how *Vibrio* community composition responds to temperature fluctuations in natural environments, we investigated the thermal niche distribution among phylogenetically distinct strains. We selected 14 representative isolates based on their ecological and phylogenetic significance. These strains were strategically chosen to represent the three major habitat types identified in our AdaptML analysis: 4 strains from habitat H_A (H_A1-4, representing clade 13), which showed adaptation to higher salinity marine conditions; 4 strains from habitat H_B (H_B1-4, representing clade 12), which demonstrated a preference for estuarine conditions; and 6 strains from habitat H_C (H_C1-6, representing clade 10), which exhibited distinct cool-temperature adaptations (Table S2). This selection enabled a direct comparison of thermal performance across ecologically differentiated populations while controlling for phylogenetic relationships. Growth rates were measured across temperatures from 8° to 52°C at 4°C intervals.

The thermal performance curves revealed distinct physiological adaptations among the clades (Figure 6). H_C strains demonstrated a narrower temperature range but exhibited measurable growth at 8°C, suggesting even lower temperature tolerance limits beyond our experimental range. In contrast, H_A and H_B strains showed no growth at 8°C but thrived at temperatures between 32° and 36°C—conditions lethal to H_C strains, reflecting thermal niche partitioning previously observed in *Vibrionaceae* (Yung et al. 2015). This clear thermal partitioning, marked by an 8°C difference in T_{opt} between H_A/H_B and H_C strains, aligned with their distribution patterns in natural environments (Baker-Austin et al. 2013).

While H_A and H_B strains displayed optimal growth at 36°–40°C, consistent with mesophilic *Vibrio* physiology, these

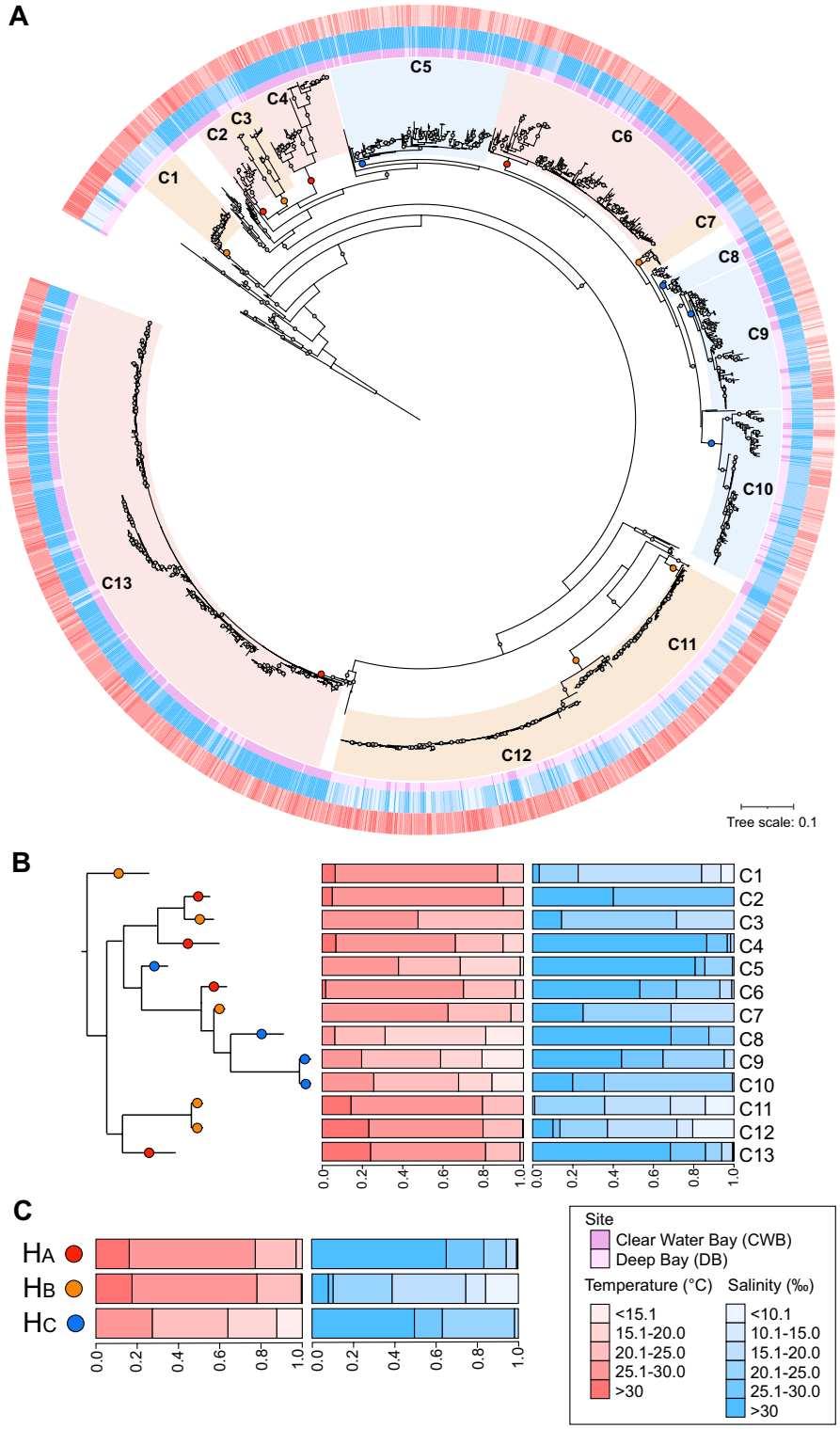

FIGURE 5 | Environmental distributions and habitat analysis of Vibrio populations across contrasting coastal environments based on Hsp60 gene phylogeny. (A) Maximum likelihood phylogenetic tree employing the LG + F + R4 model showing the relationship between Vibrio isolates. The innermost ring (purple) indicates sampling sites (CWB and DB), followed by a ring showing salinity distributions (blue, ranging from < 10.1‰ to > 30‰), and an outermost ring displaying temperature distributions (red, ranging from < 15.1° to > 30°C). Grey dots indicate nodes with bootstrap support values greater than 0.9. The tree scale bar represents 0.1 nucleotide substitutions per site. (B) Distribution profiles of identified clades (C1-C13) across different temperature (red) and salinity (blue) ranges. The distributions are plotted in 5°C temperature bins (< 15.1° to > 30°C) and 5‰ salinity bins (< 10.1‰ to > 30‰), with relative abundance normalised on a scale from 0.0 to 1.0 to account for sampling effort. (C) Distribution profiles of AdaptML-predicted habitats (HA, HB, HC) showing the relative abundance of each habitat type across temperature and salinity gradients. Values are normalised on a scale from 0.0 to 1.0 to account for sampling effort, revealing distinct ecological preferences among the three predicted habitat types.

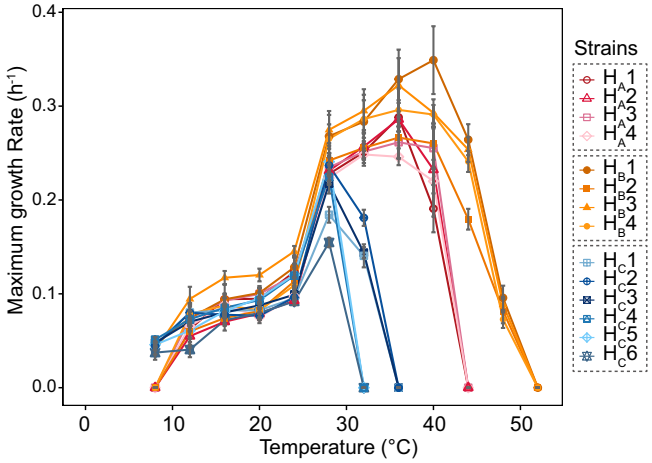

FIGURE 6 | Maximum growth rates of 14 *Vibrio* strains across a temperature gradient. The figure shows the maximum growth rates (h^{-1}) of 14 distinct Vibrio strains (H_A1–H_A4, H_B1–H_B4, H_C1–H_C6) measured at different temperatures (0°–50°C).

temperatures exceed typical marine conditions, suggesting potential adaptation to warm-blooded hosts. This thermal tolerance pattern indicates that H_A and H_B strains, particularly *V. parahaemolyticus* (H_B1-2) and *V. harveyi* (H_A1-2), might include potential human pathogens (Baker-Austin et al. 2013). In contrast, H_C strains, including *V. crassostreae* (H_C3-6), were unable to survive at 36°C, suggesting better adaptation as pathogens of marine organisms such as oysters and fish.

A particularly significant finding emerged from our analysis of *V. alginolyticus* strains (H_B3-4 and H_C1-2), which shared >97% sequence similarity in their Hsp60 genes yet exhibited markedly different thermal adaptations. Despite belonging to the same species by conventional molecular taxonomy, these strains were distributed across distinct phylogenetic clades (12 and 10) and displayed contrasting physiological characteristics.

H_B3-4 showed a higher temperature optima characteristic of habitat H_B, while H_C1-2 exhibited the lower temperature preferences typical of habitat H_C strains.

This observation represents a compelling example of fine-scale adaptive divergence within a single species, where temperature-driven selection has promoted rapid physiological differentiation while conserved molecular markers remain largely unchanged. The maintenance of distinct thermal ecotypes within *V. alginolyticus* suggests that environmental adaptation can precede substantial genetic divergence in housekeeping genes, likely representing an early stage in bacterial speciation, where populations begin occupying distinct environmental niches while maintaining genetic cohesion across most of their genome. Such findings challenge traditional species concepts in bacteria and highlight the importance of considering ecological adaptation alongside molecular markers when examining bacterial diversity.

The hierarchical organisation of environmental influences revealed by our analysis suggests salinity acts as the primary driver of population differentiation between H_A and H_B populations, while temperature plays a crucial role in defining H_C strains regardless of salinity conditions. This pattern indicates a complex interaction between these environmental parameters in structuring *Vibrio* communities, where different populations employ distinct strategies for environmental adaptation. Our findings demonstrate that *Vibrio* populations employ diverse environmental adaptation strategies in coastal ecosystems: some populations show strict salinity preferences (H_A—stenohaline marine, H_B—lower salinity estuarine), while others maintain broad salinity tolerance while specialising in temperature ranges (H_C—psychrophilic generalist). The clear habitat partitioning identified through AdaptML provides strong evidence for the coexistence of these different adaptive strategies, suggesting that both temperature and salinity act as selective forces but can operate independently in structuring Vibrio populations.

3.12 | Comparative Analysis of Culture-Dependent and Culture-Independent Methods in Characterising *Vibrio* Communities

Our dual methodological approach revealed complementary yet distinct patterns in the recovery and representation of *Vibrio* populations across the sampling sites. Phylogenetic analysis of partial Hsp60 gene sequences from both ASVs and isolates identified 28 major species clusters, highlighting both the overlaps and gaps between methods. Culture-dependent methods successfully recovered numerous species, including *V. campbellii*, *V. owensii*, *V. alginolyticus*, *V. parahaemolyticus*, and *V. fortis* (Figure 7). However, they notably failed to recover several abundant species detected through amplicon sequencing, particularly *V. navarrensis*, *V. natriegens*, and *V. mimicus*.

While TCBS agar provided selective isolation of *Vibrio* species, we acknowledge this introduces biases affecting our ecological differentiation interpretation. TCBS selective agents may inhibit environmentally stressed or metabolically specialised Vibrio strains, including those in viable but non-culturable states or with slower growth rates (Alam et al. 2001). Media-based competition may also suppress species with lower competitive fitness under laboratory conditions (Weichart and Kjelleberg 1996). This cultivation bias likely explains why several *Vibrio* populations detected in our amplicon sequencing analysis remained uncultured, potentially underrepresenting their ecological niches in our differentiation analysis.

A particularly significant finding emerged from our phylogenetic analysis: uncultivated *Vibrio* species showed closer genetic relationships to each other (Figure 7). This pattern, exemplified by *V. navarrensis* and its relatives, suggests that cultivability on TCBS may be influenced by shared genetic determinants. Previous studies characterising *V. cidicii* found that *V. navarrensis* was its closest relative, forming a distinct lineage within the *Vibrio* phylogeny (Orata et al. 2016). This clustering of uncultivable strains suggests common genetic factors may influence adaptability to selective agents or competitive ability under culture conditions. Our analysis also revealed complexity in *Vibrio* molecular taxonomy through the presence of multiple copies of the Hsp60 gene. Several species, including *V. alginolyticus*, *V. parahaemolyticus*, and *V. natriegens*, showed two distinct clades with low Hsp60 gene sequence similarity (<90%). These differences corresponded to distinct Hsp60 gene copies

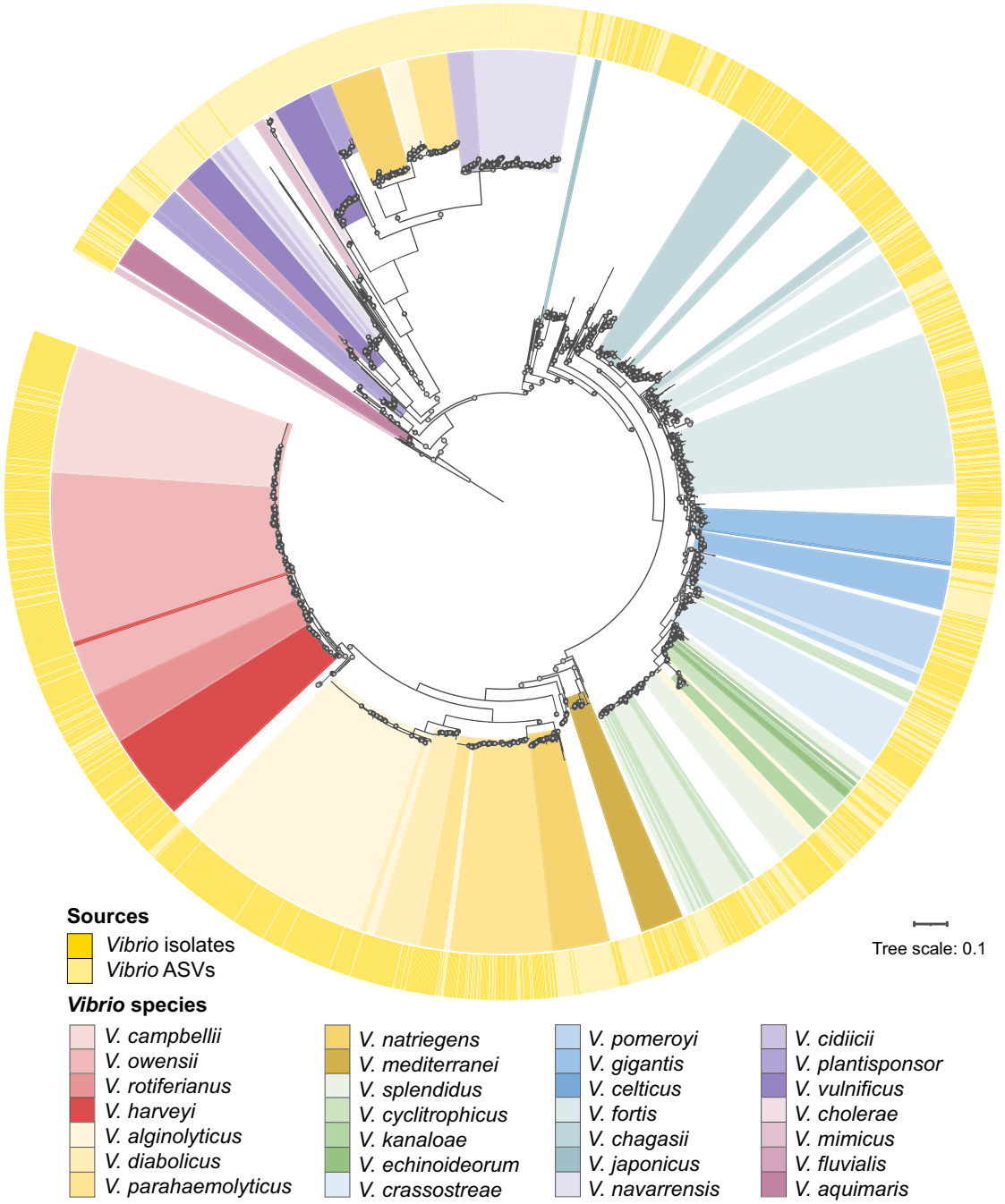

FIGURE 7 | Phylogenetic distribution of *Vibrio* species identified based on Hsp60 gene sequences. A Maximum Likelihood tree was constructed using IQTree employing the LG + F + R4 model and visualised with isolation temperatures in iTOL. The tree shows the taxonomic diversity of Vibrio species detected in the Pearl River Estuary, with a scale bar representing 0.1 nucleotide substitutions per site. The outer ring indicates the source of detection, distinguishing between cultured Vibrio isolates and Vibrio ASVs (amplicon sequence variants).

located on chromosomes 1 and 2 of the *Vibrio* genome, confirming previous findings (King et al. 2019). Chromosome 2 copies were exclusively detected through ASV methods, likely due to primer differences (Table S3), highlighting how methodological choices can influence taxonomic identification and diversity assessments.

The bias introduced by TCBS agar has important implications for interpreting ecological differentiation among *Vibrio* species. While culture-dependent methods provide valuable insights into the physiology and functional traits of isolated species, their selective nature likely underrepresents the diversity and ecological roles of uncultured taxa. Amplicon sequencing, in contrast, captures a broader spectrum of *Vibrio* diversity, including species that may play critical roles in their native environments but are excluded from culture-based analyses. Together, these findings emphasise the need for an integrative approach that combines culture-dependent and culture-independent methods

to achieve a more comprehensive understanding of *Vibrio* community structure and ecological differentiation.

4 | Conclusions

Our comprehensive analysis of *Vibrio* populations in contrasting coastal environments reveals a complex interplay between environmental factors and bacterial adaptation at multiple ecological scales. By integrating culture-dependent and molecular approaches, we demonstrate that salinity acts as the primary driver of community differentiation between estuarine and coastal waters, while temperature orchestrates seasonal succession patterns.

The estuarine environment of Deep Bay exhibited higher bacterial abundance and diversity, with more pronounced seasonal community shifts compared to the relatively stable coastal waters of Clear Water Bay, illustrating how environmental heterogeneity shapes microbial community structure and drives ecological diversification. The distinct physicochemical profiles of each site—DB's dynamic, nutrient-rich conditions versus CWB's stable, oligotrophic environment—created selective pressures that fostered different adaptive strategies among *Vibrio* populations.

A key finding emerged from our phylogenetic analysis of *Vibrio* isolates, which revealed three distinct ecological habitats defined by specific combinations of temperature and salinity preferences. Habitat H_A (predominantly CWB strains) showed stenohaline adaptation to higher salinity conditions, while Habitat H_B (mainly DB strains) displayed greater euryhalinity in moderate to lower salinity environments. Habitat H_C revealed a specialised adaptation to cooler temperatures while maintaining broad salinity tolerance—a distinct ecological strategy allowing these strains to persist across diverse coastal environments during winter months.

Particularly significant was our discovery of distinct thermal adaptations among *V. alginolyticus* strains sharing high genetic similarity (> 97% Hsp60 gene sequence identity). This finding demonstrates that ecological specialisation can precede substantial genetic divergence in housekeeping genes, challenging traditional species concepts in bacterial taxonomy and suggesting rapid adaptive responses to environmental conditions. The maintenance of distinct thermal ecotypes within the same species represents an early stage in bacterial speciation, where populations begin occupying different environmental niches while maintaining genetic cohesion across most of their genome.

Our dual methodological approach uncovered important technical biases, with several abundant species detected through amplicon sequencing (particularly *V. navarrensis*, *V. natriegens*, and *V. mimicus*) remaining uncultivable using standard methods. The clustering of these uncultivated species in distinct phylogenetic clades suggests shared genetic determinants influencing cultivability and highlights the importance of combining multiple approaches for comprehensive community characterisation.

These findings advance our understanding of how environmental heterogeneity drives fine-scale population differentiation in marine bacteria and provide a framework for predicting Vibrio population responses to environmental change. The clear thermal specialisation patterns observed have particular relevance for anticipating shifts in pathogenic Vibrio distributions under climate change scenarios, especially in subtropical coastal systems where warming trends may favour certain ecotypes over others. This work establishes a foundation for improved monitoring strategies in coastal environments and highlights the importance of considering both broad community patterns and strain-level adaptations in microbial ecology studies.

Author Contributions

Siu Hei Wan: writing – original draft, visualization, validation, methodology, investigation, formal analysis, data curation, conceptualization. **Yangbing Xu:** writing – review and editing, methodology, investigation, data curation, visualization. **Wenqian Xu:** investigation, methodology, visualization, writing – review and editing, data curation. **Shara K. K. Leung:** methodology, investigation, data curation. **Erin Y. N. Yu:** methodology, investigation, data curation. **Charmaine C. M. Yung:** conceptualization, writing – review and editing, funding acquisition, project administration, supervision, resources, formal analysis, visualization.

Acknowledgements

This research was supported by funding from the Research Grants Council of Hong Kong (Project Reference Number: AoE/P-601/23-N). We extend our sincere gratitude to Mr. Woo Chun Fai and Mr. Samuel Cheng for their invaluable logistical support throughout this project.

Conflicts of Interest

The authors declare no conflicts of interest.

Data Availability Statement

All sequencing data has been deposited to NCBI database under accession number PRJNA1233806.

References

Alam, M. J., K. Tomochika, S. Miyoshi, and S. Shinoda. 2001. "Analysis of Seawaters for the Recovery of Culturable Vibrio Parahaemolyticus and Some Other Vibrios." *Microbiology and Immunology* 45: 393–397.

Avendaño, K. A., S. J. Ponce-Jahen, E. I. Valenzuela, et al. 2024. "Nitrogen Loss in Coastal Sediments Driven by Anaerobic Ammonium Oxidation Coupled to Microbial Reduction of Mn(IV)-Oxide." *Science of the Total Environment* 923: 171368.

Baker-Austin, C., J. A. Trinanes, N. G. H. Taylor, R. Hartnell, A. Siitonen, and J. Martinez-Urtaza. 2013. "Emerging Vibrio Risk at High Latitudes in Response to Ocean Warming." *Nature Climate Change* 3: 73–77.

Bolyen, E., J. R. Rideout, M. R. Dillon, et al. 2019. "Reproducible, Interactive, Scalable and Extensible Microbiome Data Science Using QIIME 2." *Nature Biotechnology* 37: 852–857.

Brumfield, K. D., M. Usmani, S. Santiago, et al. 2023. "Genomic Diversity of Vibrio spp. and Metagenomic Analysis of Pathogens in Florida Gulf Coastal Waters Following Hurricane Ian." *MBio* 14, no. 6: e01476-23. https://doi.org/10.1128/mbio.01476-23.

Bruto, M., A. James, B. Petton, et al. 2017. "*Vibrio crassostreae*, A Benign Oyster Colonizer Turned Into a Pathogen After Plasmid Acquisition." *ISME Journal* 11: 1043–1052.

Buchan, A., J. M. González, and M. A. Moran. 2005. "Overview of the Marine Roseobacter Lineage." *Applied and Environmental Microbiology* 71: 5665–5677.

Bunse, C., and J. Pinhassi. 2017. "Marine Bacterioplankton Seasonal Succession Dynamics." *Trends in Microbiology* 25: 494–505.

Callbeck, C. M., C. Pelzer, G. Lavik, et al. 2019. "Arcobacter Peruensis sp. Nov., a Chemolithoheterotroph Isolated From Sulfide- and Organic-Rich Coastal Waters Off Peru." *Applied and Environmental Microbiology* 85, no. 24: e01344-19. https://doi.org/10.1128/AEM.01344-19.

Capella-Gutiérrez, S., J. M. Silla-Martínez, and T. Gabaldón. 2009. "trimAl: A Tool for Automated Alignment Trimming in Large-Scale Phylogenetic Analyses." *Bioinformatics* 25: 1972–1973.

Ceccarelli, D., and R. R. Colwell. 2014. "Vibrio Ecology, Pathogenesis, and Evolution." *Frontiers in Microbiology* 5: 256.

Chowdhury, M. A., H. Yamanaka, S. Miyoshi, K. M. Aziz, and S. Shinoda. 1989. "Ecology of *Vibrio mimicus* in Aquatic Environments." *Applied and Environmental Microbiology* 55: 2073–2078.

Cloern, J. E., S. Q. Foster, and A. E. Kleckner. 2014. "Phytoplankton Primary Production in the World's Estuarine-Coastal Ecosystems." *Biogeosciences* 11: 2477–2501.

Corzett, C. H., J. Elsherbini, D. M. Chien, et al. 2018. "Evolution of a Vegetarian Vibrio: Metabolic Specialization of *Vibrio breoganii* to Macroalgal Substrates." *Journal of Bacteriology* 200, no. 15: 10–1128. https://doi.org/10.1128/jb.00020-18.

Crump, B. C., C. S. Hopkinson, M. L. Sogin, and J. E. Hobbie. 2004. "Microbial Biogeography Along an Estuarine Salinity Gradient: Combined Influences of Bacterial Growth and Residence Time." *Applied and Environmental Microbiology* 70: 1494–1505.

de Souza Valente, C., and A. H. L. Wan. 2021. "Vibrio and Major Commercially Important Vibriosis Diseases in Decapod Crustaceans." *Journal of Invertebrate Pathology* 181: 107527.

Dixon, P. 2003. "VEGAN, a Package of R Functions for Community Ecology." *Journal of Vegetation Science* 14: 927–930.

Duarte, C. M., I. E. Hendriks, T. S. Moore, et al. 2013. "Is Ocean Acidification an Open-Ocean Syndrome? Understanding Anthropogenic Impacts on Seawater pH." *Estuaries and Coasts* 36: 221–236.

Edgar, R. C. 2004. "MUSCLE: Multiple Sequence Alignment With High Accuracy and High Throughput." *Nucleic Acids Research* 32: 1792–1797.

Edgar, R. C. 2013. "UPARSE: Highly Accurate OTU Sequences From Microbial Amplicon Reads." *Nature Methods* 10: 996–998.

Edgar, R. C., and H. Flyvbjerg. 2015. "Error Filtering, Pair Assembly and Error Correction for Next-Generation Sequencing Reads." *Bioinformatics* 31: 3476–3482.

Erken, M., C. Lutz, and D. McDougald. 2015. "Interactions of Vibrio spp. With Zooplankton." *Microbiology Spectrum* 3: 128. https://doi.org/10.1128/microbiolspec.ve-0003-2014.

Francis, T. B., K. Krüger, B. M. Fuchs, H. Teeling, and R. I. Amann. 2019. "*Candidatus* Prosiliicoccus Vernus, a Spring Phytoplankton Bloom Associated Member of the *Flavobacteriaceae*." *Systematic and Applied Microbiology* 42: 41–53.

Fuhrman, J. A., J. A. Cram, and D. M. Needham. 2015. "Marine Microbial Community Dynamics and Their Ecological Interpretation." *Nature Reviews. Microbiology* 13: 133–146.

Gao, P., N. Q. I. Mohd Noor, and S. Md. Shaarani. 2022. "Current Status of Food Safety Hazards and Health Risks Connected With Aquatic Food Products From Southeast Asian Region." *Critical Reviews in Food Science and Nutrition* 62: 3471–3489.

Garrido-Maestu, A., A. Lozano-León, R. R. Rodríguez-Souto, R. Vieites-Maneiro, M.-J. Chapela, and A. G. Cabado. 2016. "Presence of Pathogenic *Vibrio* Species in Fresh Mussels Harvested in the Southern Rias of Galicia (NW Spain)." *Food Control* 59: 759–765.

Gilbert, J. A., J. A. Steele, J. G. Caporaso, et al. 2012. "Defining Seasonal Marine Microbial Community Dynamics." *ISME Journal* 6: 298–308.

Gladney, L. M., and C. L. Tarr. 2020. "Molecular and Phenotypic Characterization of *Vibrio Navarrensis* Isolates Associated With Human Illness." *Journal of Clinical Microbiology* 52: 4070–4074.

Goh, S. H., S. Potter, J. O. Wood, S. M. Hemmingsen, R. P. Reynolds, and A. W. Chow. 1996. "HSP60 Gene Sequences as Universal Targets for Microbial Species Identification: Studies With Coagulase-Negative Staphylococci." *Journal of Clinical Microbiology* 34: 818–823.

Gradoville, M. R., B. C. Crump, C. C. Häse, and A. E. White. 2018. "Environmental Controls of Oyster-Pathogenic Vibrio spp. in Oregon Estuaries and a Shellfish Hatchery." *Applied and Environmental Microbiology* 84: e02156-17.

Greenfield, D. I., J. Gooch Moore, J. R. Stewart, et al. 2017. "Temporal and Environmental Factors Driving Vibrio Vulnificus and *V. parahaemolyticus* Populations and Their Associations With Harmful Algal Blooms in South Carolina Detention Ponds and Receiving Tidal Creeks." *GeoHealth* 1: 306–317.

Guardiola-Avila, I., E. Acedo-Felix, I. Sifuentes-Romero, G. Yepiz-Plascencia, B. Gomez-Gil, and L. Noriega-Orozco. 2016. "Molecular and Genomic Characterization of *Vibrio mimicus* Isolated From a Frozen Shrimp Processing Facility in Mexico." *PLoS One* 11: e0144885.

Han, X., K. Beck, H. Bürgmann, B. Frey, B. Stierli, and A. Frossard. 2023. "Synthetic Oligonucleotides as Quantitative PCR Standards for Quantifying Microbial Genes." *Frontiers in Microbiology* 14: 1279041.

Harrison, P. J., K. Yin, J. H. W. Lee, J. Gan, and H. Liu. 2008. "Physical–Biological Coupling in the Pearl River Estuary." *Continental Shelf Research* 28: 1405–1415.

Hofer, U. 2018. "The Majority Is Uncultured." *Nature Reviews. Microbiology* 16: 716–717.

Hunt, D. E., L. A. David, D. Gevers, S. P. Preheim, E. J. Alm, and M. F. Polz. 2008. "Resource Partitioning and Sympatric Differentiation Among Closely Related Bacterioplankton." *Science* 320, no. 5879: 1081–1085. https://doi.org/10.1126/science.1157890.

Janecko, N., S. J. Bloomfield, R. Palau, and A. E. Mather. 2021. "Whole Genome Sequencing Reveals Great Diversity of Vibrio spp in Prawns at Retail." *Microbial Genomics* 7: 000647.

Jesser, K. J., and R. T. Noble. 2018. "*Vibrio* Ecology in the Neuse River Estuary, North Carolina, Characterized by Next-Generation Amplicon Sequencing of the Gene Encoding Heat Shock Protein 60 (*hsp60*)." *Applied and Environmental Microbiology* 84: e00333-18.

Johnson, C. N., A. R. Flowers, N. F. NorieaIII, et al. 2010. "Relationships Between Environmental Factors and Pathogenic Vibrios in the Northern Gulf of Mexico." *Applied and Environmental Microbiology* 76, no. 21: 7076–7084.

Joshi, N. A., and J. N. Fass. 2011. "Sickle: A Sliding-Window, Adaptive, Quality-Based Trimming Tool for FastQ Files".

Kalatzis, P. G., R. Bastías, C. Kokkari, and P. Katharios. 2016. "Isolation and Characterization of Two Lytic Bacteriophages, φSt2 and φGrn1; Phage Therapy Application for Biological Control of *Vibrio alginolyticus* in Aquaculture Live Feeds." *PLoS One* 11: e0151101.

Katoh, K., K. Kuma, H. Toh, and T. Miyata. 2005. "MAFFT Version 5: Improvement in Accuracy of Multiple Sequence Alignment." *Nucleic Acids Research* 33: 511–518.

Kearse, M., R. Moir, A. Wilson, et al. 2012. "Geneious Basic: An Integrated and Extendable Desktop Software Platform for the Organization and Analysis of Sequence Data." *Bioinformatics* 28: 1647–1649.

Khan, M. M. T., B. H. Pyle, and A. K. Camper. 2010. "Specific and Rapid Enumeration of Viable but Nonculturable and Viable-Culturable Gram-Negative Bacteria by Using Flow Cytometry." *Applied and Environmental Microbiology* 76: 5088–5096.

King, W. L., N. Siboni, T. Kahlke, T. J. Green, M. Labbate, and J. R. Seymour. 2019. "A New High Throughput Sequencing Assay for Characterizing the Diversity of Natural Vibrio Communities and Its Application to a Pacific Oyster Mortality Event." *Frontiers in Microbiology* 10: 2907.

Kokashvili, T., C. A. Whitehouse, A. Tskhvediani, et al. 2015. "Occurrence and Diversity of Clinically Important Vibrio Species in the Aquatic Environment of Georgia." *Frontiers in Public Health* 3: 232.

Kopprio, G. A., S. B. Neogi, H. Rashid, et al. 2020. "Vibrio and Bacterial Communities Across a Pollution Gradient in the Bay of Bengal: Unraveling Their Biogeochemical Drivers." *Frontiers in Microbiology* 11: 594.

Kumari, P., A. Poddar, P. Schumann, and S. K. Das. 2014. "*Vibrio panuliri* sp. Nov., a Marine Bacterium Isolated From Spiny Lobster, Panulirus Penicillatus and Transfer of *Vibrio ponticus* From Scophthalmi Clade to the Newly Proposed Ponticus Clade." *Research in Microbiology* 165: 826–835.

Letunic, I., and P. Bork. 2021. "Interactive Tree of Life (iTOL) v5: An Online Tool for Phylogenetic Tree Display and Annotation." *Nucleic Acids Research* 49: W293–W296.

Liang, J., J. Liu, X. Wang, et al. 2019. "Spatiotemporal Dynamics of Free-Living and Particle-Associated Vibrio Communities in the Northern Chinese Marginal Seas." *Applied and Environmental Microbiology* 85: e00217.

Links, M. G., T. J. Dumonceaux, S. M. Hemmingsen, and J. E. Hill. 2012. "The Chaperonin-60 Universal Target Is a Barcode for Bacteria That Enables De Novo Assembly of Metagenomic Sequence Data." *PLoS One* 7: e49755.

Main, C. R., L. R. Salvitti, E. B. Whereat, and K. J. Coyne. 2015. "Community-Level and Species-Specific Associations Between Phytoplankton and Particle-Associated Vibrio Species in Delaware's Inland Bays." *Applied and Environmental Microbiology* 81: 5703–5713.

Martin, M. 2011. "Cutadapt Removes Adapter Sequences From High-Throughput Sequencing Reads." *EMBnet Journal* 17: 10–12.

Martinez-Urtaza, J., J. C. Bowers, J. Trinanes, and A. DePaola. 2010. "Climate Anomalies and the Increasing Risk of *Vibrio Parahaemolyticus* and *Vibrio vulnificus* Illnesses." *Food Research International* 43: 1780–1790.

Matteucci, G., S. Schippa, G. Di Lallo, L. Migliore, and M. C. Thaller. 2015. "Species Diversity, Spatial Distribution, and Virulence Associated Genes of Culturable Vibrios in a Brackish Coastal Mediterranean Environment." *Annales de Microbiologie* 65: 2311–2321.

McLaughlin, J. B., A. DePaola, C. A. Bopp, et al. 2005. "Outbreak of *Vibrio Parahaemolyticus* Gastroenteritis Associated With Alaskan Oysters." *New England Journal of Medicine* 353, no. 14: 1463–1470. https://doi.org/10.1056/NEJMoa051594.

Meibom, K. L., X. B. Li, A. T. Nielsen, C.-Y. Wu, S. Roseman, and G. K. Schoolnik. 2004. "The *Vibrio cholerae* Chitin Utilization Program." *Proceedings of the National Academy of Sciences* 101: 2524–2529.

Minh, B. Q., H. A. Schmidt, O. Chernomor, et al. 2020. "IQ-TREE 2: New Models and Efficient Methods for Phylogenetic Inference in the Genomic Era." *Molecular Biology and Evolution* 37: 1530–1534.

Motes, M. L., A. DePaola, D. W. Cook, et al. 1998. "Influence of Water Temperature and Salinity on *Vibrio vulnificus* in Northern Gulf and Atlantic Coast Oysters (*Crassostrea virginica*)." *Applied and Environmental Microbiology* 64: 1459–1465.

Ndraha, N., H. Wong, and H.-I. Hsiao. 2020. "Managing the Risk of *Vibrio parahaemolyticus* Infections Associated With Oyster Consumption: A Review." *Comprehensive Reviews in Food Science and Food Safety* 19: 1187–1217.

Needham, D. M., and J. A. Fuhrman. 2016. "Pronounced Daily Succession of Phytoplankton, Archaea and Bacteria Following a Spring Bloom." *Nature Microbiology* 1: 1–7.

Nyholm, S. V., and M. McFall-Ngai. 2004. "The Winnowing: Establishing the Squid–Vibrio Symbiosis." *Nature Reviews. Microbiology* 2: 632–642.

Orata, F. D., Y. Xu, L. M. Gladney, et al. 2016. "Characterization of Clinical and Environmental Isolates of *Vibrio cidicii* sp. Nov., a Close Relative of *Vibrio navarrensis*." *International Journal of Systematic and Evolutionary Microbiology* 66: 4148–4155.

Orsi, W. D., J. M. Smith, S. Liu, et al. 2016. "Diverse, Uncultivated Bacteria and Archaea Underlying the Cycling of Dissolved Protein in the Ocean." *ISME Journal* 10: 2158–2173.

Paerl, H. W., N. S. Hall, and E. S. Calandrino. 2011. "Controlling Harmful Cyanobacterial Blooms in a World Experiencing Anthropogenic and Climatic-Induced Change." *Science of the Total Environment* 409: 1739–1745.

Paerl, H. W., L. M. Valdes, B. L. Peierls, J. E. Adolf, and L. W. Harding Jr. 2006. "Anthropogenic and Climatic Influences on the Eutrophication of Large Estuarine Ecosystems." *Limnology and Oceanography* 51: 448–462.

Parada, A. E., D. M. Needham, and J. A. Fuhrman. 2016. "Every Base Matters: Assessing Small Subunit rRNA Primers for Marine Microbiomes With Mock Communities, Time Series and Global Field Samples." *Environmental Microbiology* 18: 1403–1414.

Pinto, D., M. A. Santos, and L. Chambel. 2015. "Thirty Years of Viable but Nonculturable State Research: Unsolved Molecular Mechanisms." *Critical Reviews in Microbiology* 41: 61–76.

Pruzzo, C., L. Vezzulli, and R. R. Colwell. 2008. "Global Impact of *Vibrio Cholerae* Interactions With Chitin." *Environmental Microbiology* 10: 1400–1410.

Quast, C., E. Pruesse, P. Yilmaz, et al. 2013. "The SILVA Ribosomal RNA Gene Database Project: Improved Data Processing and Web-Based Tools." *Nucleic Acids Research* 41: D590–D596.

Rubio-Portillo, E., P. Yarza, C. Peñalver, A. A. Ramos-Esplá, and J. Antón. 2014. "New Insights Into *Oculina patagonica* Coral Diseases and Their Associated Vibrio spp. Communities." *ISME Journal* 8: 1794–1807.

Sampaio, A., V. Silva, P. Poeta, and F. Aonofriesei. 2022. "*Vibrio* spp.: Life Strategies, Ecology, and Risks in a Changing Environment." *Diversity* 14: 97.

Sawabe, T., Y. Fujimura, K. Niwa, and H. Aono. 2007. "*Vibrio comitans* Sp. Nov., *Vibrio rarus* sp. Nov. and *Vibrio inusitatus* sp. Nov., From the Gut of the Abalones *Haliotis discus discus*, *H. gigantea*, H. Madaka and *H. rufescens*." *International Journal of Systematic and Evolutionary Microbiology* 57: 916–922.

Sawabe, T., Y. Ogura, Y. Matsumura, et al. 2013. "Updating the Vibrio Clades Defined by Multilocus Sequence Phylogeny: Proposal of Eight New Clades, and the Description of *Vibrio tritonius* sp. Nov." *Frontiers in Microbiology* 4: 414.

Shapiro, B. J., J. Friedman, O. X. Cordero, et al. 2012. "Population Genomics of Early Events in the Ecological Differentiation of Bacteria." *Science* 336: 48–51.

Shi, R., J. Li, Z. Qi, Z. Zhang, H. Liu, and H. Huang. 2018. "Abundance and Community Composition of Bacterioplankton in the Northern South China Sea During Winter: Geographic Position and Water Layer Influences." *Biologia* 73: 197–206.

Sogin, M. L., H. G. Morrison, J. A. Huber, et al. 2006. "Microbial Diversity in the Deep Sea and the Underexplored "Rare Biosphere"." *Proceedings of the National Academy of Sciences of the United States of America* 103: 12115–12120.

Sunagawa, S., L. P. Coelho, S. Chaffron, et al. 2015. "Structure and Function of the Global Ocean Microbiome." *Science* 348: 1261359.

Takemura, A., D. Chien, and M. Polz. 2014. "Associations and Dynamics of Vibrionaceae in the Environment, From the Genus to the Population Level." *Frontiers in Microbiology* 5: 38.

Tee, H. S., D. Waite, G. Lear, and K. M. Handley. 2021. "Microbial River-To-Sea Continuum: Gradients in Benthic and Planktonic Diversity, Osmoregulation and Nutrient Cycling." *Microbiome* 9: 190.

Teeling, H., B. M. Fuchs, C. M. Bennke, et al. 2016. "Recurring Patterns in Bacterioplankton Dynamics During Coastal Spring Algae Blooms." *eLife* 5: e11888.

Thompson, F. L., Y. Li, B. Gomez-Gil, et al. 2003. "*Vibrio neptunius* Sp. Nov., *Vibrio brasiliensis* sp. Nov. and *Vibrio xuii* sp. Nov., Isolated From the Marine Aquaculture Environment (Bivalves, Fish, Rotifers and Shrimps)." *International Journal of Systematic and Evolutionary Microbiology* 53: 245–252.

Thompson, J. R., M. A. Randa, L. A. Marcelino, A. Tomita-Mitchell, E. Lim, and M. F. Polz. 2004. "Diversity and Dynamics of a North Atlantic Coastal Vibrio Community." *Applied and Environmental Microbiology* 70: 4103–4110.

Vezzulli, L., C. Grande, P. C. Reid, et al. 2016. "Climate Influence on Vibrio and Associated Human Diseases During the Past Half-Century in the Coastal North Atlantic." *Proceedings of the National Academy of Sciences* 113, no. 34: E5062–E5071. https://doi.org/10.1073/pnas.1609157113.

Wang, H., F. Chen, C. Zhang, M. Wang, and J. Kan. 2021. "Estuarine Gradients Dictate Spatiotemporal Variations of Microbiome Networks in the Chesapeake Bay." *Environmental Microbiomes* 16: 22.

Wang, X., J. Liu, J. Liang, H. Sun, and X.-H. Zhang. 2020. "Spatiotemporal Dynamics of the Total and Active Vibrio spp. Populations Throughout the Changjiang Estuary in China." *Environmental Microbiology* 22: 4438–4455.

Ward, C. S., C.-M. Yung, K. M. Davis, et al. 2017. "Annual Community Patterns Are Driven by Seasonal Switching Between Closely Related Marine Bacteria." *ISME Journal* 11: 1412–1422.

Weichart, D., and S. Kjelleberg. 1996. "Stress Resistance and Recovery Potential of Culturable and Viable but Nonculturable Cells of *Vibrio vulnificus*." *Microbiology* 142: 845–853.

Westrich, J. R., A. M. Ebling, W. M. Landing, et al. 2016. "Saharan Dust Nutrients Promote Vibrio Bloom Formation in Marine Surface Waters." *Proceedings of the National Academy of Sciences* 113: 5964–5969.

Whitesides, M. D., and J. D. Oliver. 1997. "Resuscitation of *Vibrio vulnificus* From the Viable but Nonculturable State." *Applied and Environmental Microbiology* 63: 1002–1005.

Wickham, H. 2011. "ggplot2." *WIREs Computational Statistics* 3: 180–185.

Xu, H. S., N. Roberts, F. L. Singleton, R. W. Attwell, D. J. Grimes, and R. R. Colwell. 1982. "Survival and Viability of Nonculturable *Escherichia coli* and *Vibrio cholerae* in the Estuarine and Marine Environment." *Microbial Ecology* 8, no. 4: 313–323. https://doi.org/10.1007/BF02010671.

Xu, J., K. Yin, J. H. W. Lee, et al. 2010. "Long-Term and Seasonal Changes in Nutrients, Phytoplankton Biomass, and Dissolved Oxygen in Deep Bay, Hong Kong." *Estuaries and Coasts* 33: 399–416.

Xu, W., L. Gong, S. Yang, et al. 2020. "Spatiotemporal Dynamics of Vibrio Communities and Abundance in Dongshan Bay, South of China." *Frontiers in Microbiology* 11: 575287. https://doi.org/10.3389/fmicb.2020.575287.

Xu, W., Y. Xu, R. Sun, et al. 2024. "Revealing the Intricate Temporal Dynamics and Adaptive Responses of Prokaryotic and Eukaryotic Microbes in the Coastal South China Sea." *Science of the Total Environment* 952: 176019.

Yang, M., Y. Liang, S. Huang, et al. 2020. "Isolation and Characterization of the Novel Phages vB_VpS_BA3 and vB_VpS_CA8 for Lysing *Vibrio parahaemolyticus*." *Frontiers in Microbiology* 11: 259.

Yildiz, F. H., and K. L. Visick. 2009. "Vibrio Biofilms: So Much the Same Yet So Different." *Trends in Microbiology* 17: 109–118.

Yin, K., J. Zhang, P.-Y. Qian, et al. 2004. "Effect of Wind Events on Phytoplankton Blooms in the Pearl River Estuary During Summer." *Continental Shelf Research* 24: 1909–1923.

Yung, C.-M., M. K. Vereen, A. Herbert, et al. 2015. "Thermally Adaptive Tradeoffs in Closely Related Marine Bacterial Strains." *Environmental Microbiology* 17: 2421–2429.

Zhou, Z., H. Meng, Y. Liu, J.-D. Gu, and M. Li. 2017. "Stratified Bacterial and Archaeal Community in Mangrove and Intertidal Wetland Mudflats Revealed by High Throughput 16S rRNA Gene Sequencing." *Frontiers in Microbiology* 8: 2148.

Zhu, J., K. Cheng, G. Chen, J. Zhou, and Z. Cai. 2022. "Complete Genome Sequence of *Vibrio Maritimus* BH16, a Siderophore-Producing Mutualistic Bacterium Isolated From Diatom *Skeletonema costatum*." *Molecular Plant-Microbe Interactions* 35, no. 8: 723–726. https://doi.org/10.1094/MPMI-01-22-0025-A.

Zong, Y., A. C. Kemp, F. Yu, J. M. Lloyd, G. Huang, and W. W.-S. Yim. 2010. "Diatoms From the Pearl River Estuary, China and Their Suitability as Water Salinity Indicators for Coastal Environments." *Marine Micropaleontology* 75: 38–49.

Supporting Information

Additional supporting information can be found online in the Supporting Information section.